Ab Initio Study of the Thermal Isomerization of Tricyclo[3.1.0.0^{2,6}]hexane to (*Z*,*Z*)-1,3-Cyclohexadiene through the (*E*,*Z*)-1,3-Cyclohexadiene Intermediate

Steven R. Davis,*,† Kiet A. Nguyen,‡ Koop Lammertsma,§ Daniell L. Mattern,† and James E. Walker†

Department of Chemistry and Biochemistry, University of Mississippi, University, Mississippi 38677, Air Force Research Laboratory, Materials and Manufacturing Directorate AFRL/MLPJ, Wright-Patterson Air Force Base, Dayton, Ohio 45433-7702, and Department of Chemistry De Boelelaan, Vrije Universiteit, FEW, 1083, 1081 HV Amsterdam, The Netherlands

Received: October 11, 2002

The isomerization of tricyclo[3.1.0.0^{2,6}]hexane to 1,3-cyclohexadiene was studied using ab initio calculations at the multiconfiguration and single-configuration levels of theory. Single-point energy calculations were also performed using the MCQDPT2 and CCSD(T) methods. The isomerization process was found to proceed through an (*E*,*Z*)-1,3-cyclohexadiene intermediate following a concerted, asynchronous pathway characterized as a conrotatory ring opening of the bicyclobutane moiety. The second step involves rotation about the trans double bond resulting in the (*Z*,*Z*)-1,3-cyclohexadiene product. The rate determining step is the first one, with an activation barrier of about 43 kcal mol^{-1}. The activation barrier of the second step was found to be only 3 kcal mol^{-1}. A second concerted pathway was found leading directly to (*Z*,*Z*)-1,3-cyclohexadiene but with an activation barrier of 54 kcal mol^{-1}. A multiconfiguration based wave function is necessary to properly describe the potential energy surface of the reaction.

Introduction

Thermal pericyclic rearrangements have received considerable interest in light of the various pathways possible. For example, the thermal rearrangement of the simple model compound bicyclobutane(**1**) to form 1,3-butadiene(**2**) has been studied both experimentally and theoretically. Possible pathways include concerted synchronous,[1] concerted asynchronous,[2,3] and nonconcerted biradical[4] mechanisms. Among the theoretical results, Dewar and Kirschner[4] argued for a nonconcerted pathway involving the propylcarbinyl biradical intermediate(**3**), based on semiempirical methods. Ab initio methods have been performed[2,3] which support a concerted asynchronous mechanism with a transition state containing partial biradical character. In a recent paper by Nguyen and Gordon,[3] various pathways were examined at the multiconfiguration self-consistent field level and the lowest energy transition state was found to be one for a concerted, asynchronous, conrotatory ring opening leading directly to butadiene. The calculated activation barrier of 41.5 kcal mol^{-1} agrees closely with the experimental value[5] of 40.6 kcal mol^{-1}. The disrotatory ring opening pathway was calculated to have a transition state about 15 kcal·mol^{-1} higher than that for the conrotatory ring opening.

Although conrotatory and disrotatory products cannot be distinguished experimentally for **1**, the exo,exo-dimethylated analogue **4** does in fact give[6] the (*E*,*Z*) isomerization product **5** expected for conrotation of the two methylene groups (that is, one exo CH_3 group rotates away from its adjacent breaking bond, whereas the other exo CH_3 group rotates toward its adjacent breaking bond[7]). This result is consistent with the Woodward−Hoffmann orbital symmetry rules, which predict[8] an allowed [σ2s+σ2a] conrotation process. A transition state orbital symmetry analysis[9] (**6**) shows that the reaction is allowed (4n electrons, Möbius topology) for such a conrotatory opening.

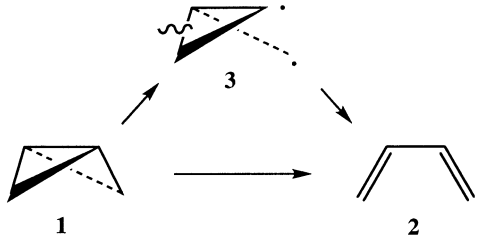

A related molecule based on the bicyclobutane structure is dihydrobenzvalene, or tricyclo[3.1.0.0^{2,6}]hexane (**7**), in which a $-CH_2CH_2-$ unit bridges the two methylene carbons of **1**. This structure is interesting because of its inherent strain energy and the effect the two-carbon bridge will have on its isomerization pathway. Experimental data for the strain energy and heat of formation for this structure are not available, but we, and others, have reported these values as determined from ab initio methods.[10−12] The strain energy of **7** was found to be slightly higher than that of **1** (66.9 kcal mol^{-1}), with a value of 71.3 kcal mol^{-1}, and a heat of formation of 57.3 kcal mol^{-1}.

The thermal decomposition of **7** has been reported in the gas phase by Christl and Bruntrup[13] in which a thermolysis temperature of 400 °C resulted in (*Z*,*Z*)-1,3-cyclohexadiene (**8**) as the sole product. Thermolysis in solution[14] also produced **8** with a measured activation barrier of 41.7 kcal mol^{-1}. Two possible mechanisms were discussed[13] in which the isomerization could initially proceed either through a true biradical intermediate (**11**) or through the intermediate (*E*,*Z*)-1,3-cyclohexadiene (**9**). However, the authors did not suggest that **9** would lead directly to **8**, but rather, by electrocyclic ring opening, to

* To whom correspondence should be addressed.
† University of Mississippi.
‡ Wright-Patterson Air Force Base.
§ Vrije Universiteit.

10.1021/jp027188o CCC: $25.00
Published on Web 12/11/2002

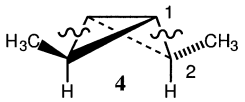

4

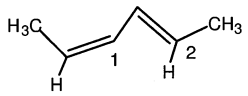

5

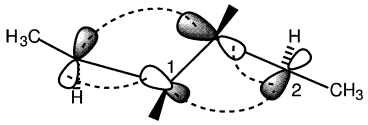

6

1,3,5-hexatriene (**10**), which could then undergo electrocyclic ring closure to give **8**. Both Christl et al.,[14] and Wiberg et al.,[15] proposed the homologous (*E*,*Z*)-1,3-cycloheptadiene (**13**) to be an intermediate in the formation of bicyclo[3.2.0]hept-6-ene (**14**) from tricyclo[4.1.0.0^{2,7}]heptane (**12**).

The possibility of the isomerization of **7** occurring through **9** is interesting in light of the apparent highly strained nature of a six-carbon diene ring with a trans double bond. Such a structure might be expected to inhibit the conrotatory pathway favored for **1** → **2**. Although the existence of **9** has been postulated as an intermediate, no computational studies have been published. However, there have been computational studies regarding the structure of (*E*)-cyclohexene and its rearrangement to (*Z*)-cyclohexene. Johnson and DiRico[16] located the transition state for rotation about the trans double bond and reported an activation barrier of only 10.6 kcal mol^{-1} at the TCSCF/6−31(d) level. Later calculations at the UB3LYP/6-31G(d) level gave 9.1 kcal mol^{-1} for the isomerization barrier.[17] In light of this result, **9** could have an even lower barrier to trans double bond rotation and be a viable pathway directly to **8** instead of through **10**.

This study will report results found by following the reaction pathway in which **7** isomerizes to produce **8**.

Computational Methods

Because the transition states are expected to have substantial biradical character, the multiconfiguration self-consistent field method has been employed. Calculations were performed using the GAMESS[18] and Gaussian 98[19] suite of programs. Geometries were optimized using the 6-31G(d,p) basis set,[20] employing analytic first derivatives, whereas harmonic frequencies were determined using second derivatives computed from finite differences of the analytic first derivatives. Single-point corrections to the MCSCF energies were obtained using second-order mutliconfigurational quasidegenerate perturbation theory (MCQDPT2)[21,22] also with the 6-31G(d,p) basis set. The choice of the correct active space is critical in a MCSCF calculation as convergence to an undesired minimum in the wave function space can easily occur. In performing geometry optimizations and transition state searches, one must be certain that the resulting wave function also spans the initially chosen active space. In the calculations reported here, the active space was chosen by localizing the hartree-fock orbitals using the Boys method[23] and the appropriate bonding and virtual orbitals selected for inclusion in the active space. For **7**, the MCSCF

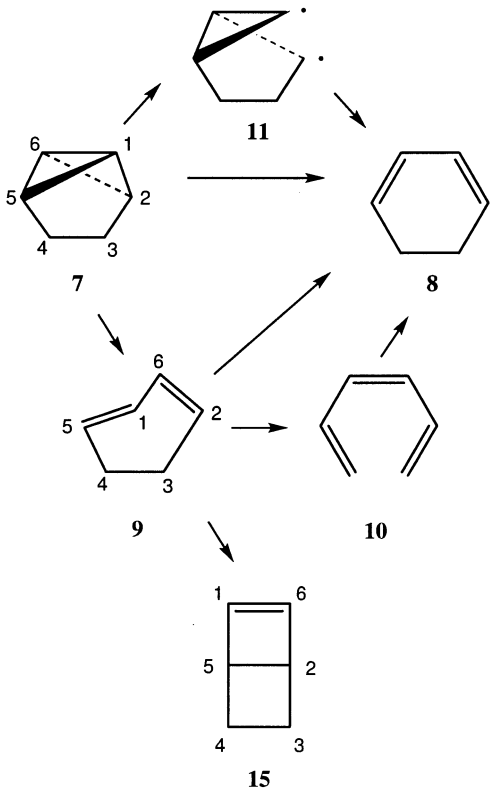

active orbitals consisted of the five occupied and five virtual C−C MO's comprising the bicyclobutane moiety, namely, the C1−C2, C1−C5, C1−C6, C2−C6, and C5−C6 bonds. For the cyclohexadienes, the bonding orbitals included the C1═C5 and C2═C6 π bonds plus the C1−C5, C2−C6, and C1−C6 σ bonds. This gives an active space consisting of 10 electrons in 10 orbitals, MCSCF(10,10). Geometries were classified as either minima or transition states by computing the harmonic frequencies. The minima have all real frequencies, whereas the transition states have a single imaginary frequency. The intrinsic reaction coordinate (IRC)[24,25] was followed in both directions from each transition state to verify the connection between the reactant and product.

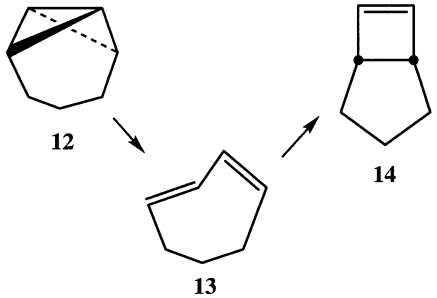

The single-determinant calculations were performed with the inclusion of electron correlation correction at the MP2[26] and CCSD(T)[27,28] levels, and using Kohn−Sham density functional theory with Becke's three-parameter hybrid exchange-correlation functional (B3LYP)[29,30] as emplemented in the Gaussian 98 program suite. Geometries were optimized using the 6-31G-(d,p) basis set[20] using analytical first derivatives, and frequencies were determined using analytical second derivatives. Single-point energies performed at the CCSD(T) level used the 6-311G-(d,p) basis set.[31]

The strain energy of **9** was determined by using the homodesmotic reaction model.[32] In this way, each carbon atom group

in the strained structure is compared to the same group in an unstrained molecule. The presence of two double bonds necessitates using unstrained alkenes in the homodesmotic reaction. For the cis double bond, we have chosen *cis*-2-butene because there is a C−C═C−C arrangement with the two end carbons in a cis arrangement in **9**. For the trans double bond, the choice was not as easy. Even though the H−C═C−H dihedral angle for the trans double bond is 179°, almost the expected 180° for a trans double bond, the restraints of the six-membered ring contort the C−C═C−C dihedral angle to about 80°, roughly midway between that of *trans*-2-butene (180°) and *cis*-2-butene (0°). Therefore, we compared results using both *cis*-2-butene and *trans*-2-butene in the homodesmotic reaction. The CH_2 groups of **9** were compared to the CH_2 group in propane, and ethane was used to mass balance the additional methyl groups. The final reaction becomes

$$9 + 4C_2H_6 \rightarrow 2(\text{cis})CH_3CHCHCH_3 + 2CH_3CH_2CH_3 \text{ or}$$

$$9 + 4C_2H_6 \rightarrow (\text{cis})CH_3CHCHCH_3 + (\text{trans})CH_3CHCHCH_3 + 2CH_3CH_2CH_3$$

The energies of each species in the reaction were determined at the[4]QCISD(T)/6-311+G(2df,p)//MP2/6-31G(d,p) level. Zero-point energy corrections to the energies were made using harmonic frequencies calculated at the MP2/6-31G(d,p) level. The calculated strain energy is then the negative of the homodesmotic reaction energy. Enthalpies of formation were determined using the calculated strain energy and experimental enthalpies of formation of the nonstrained species.

Results and Discussion

The reactant structure **7** belongs to point group C_{2v}, and the formation of **8** occurs through cleavage of the C1−C2 and C5−C6 bonds. There are two possibilities for a concerted reaction: one in which the two bonds break simultaneously, maintaining C_2 symmetry (synchronous), and one in which the bonds break at different locations along the reaction coordinate (C_1 symmetry, asynchronous). Following the synchronous pathway led to a second-order saddle point (two imaginary frequencies), whereas following the asynchronous pathway led to a true transition state (one imaginary frequency). The structures, and selected geometric parameters, of the reactant, transition state, and product for each step are given in Figure 1, whereas energy values are given in Tables 1 and 2. The IRC for this step (supplemental information) was calculated and verifies the connection of TS1 to **7** and **9**. The asynchronous nature of the first step is illustrated in Figure 2 in which a plot of selected C−C bond lengths are given as a function of the reaction coordinate. From the values of the bond lengths leading to TS1, it can be seen that the C1−C2 bond ruptures initially, leading to the transition state structure. The C1−C2 bond length increases almost linearly up to TS1, at which it is a maximum, whereas the C5−C6 bond length remains fairly constant until very close to TS1, at which point it begins to increase substantially. Proceeding along the IRC toward the product, the second bond (C5−C6) breaks, and formation of the intermediate **9** occurs. The two double bonds are at their minimum shortly after TS1, and remain fairly constant during the final stages of the C5−C6 bond fission. One of the most interesting aspects of this reaction step is the formation of the trans double bond in the intermediate **9**. The H1−C1−C5−H5 dihedral is only 14.1° in **7** but is 166.0° in TS1. It is apparent that the trans double bond forms early on in the reaction surface, and as C1−C2 ruptures, H1 undergoes concomitant rotation toward the C3−C4 bond.

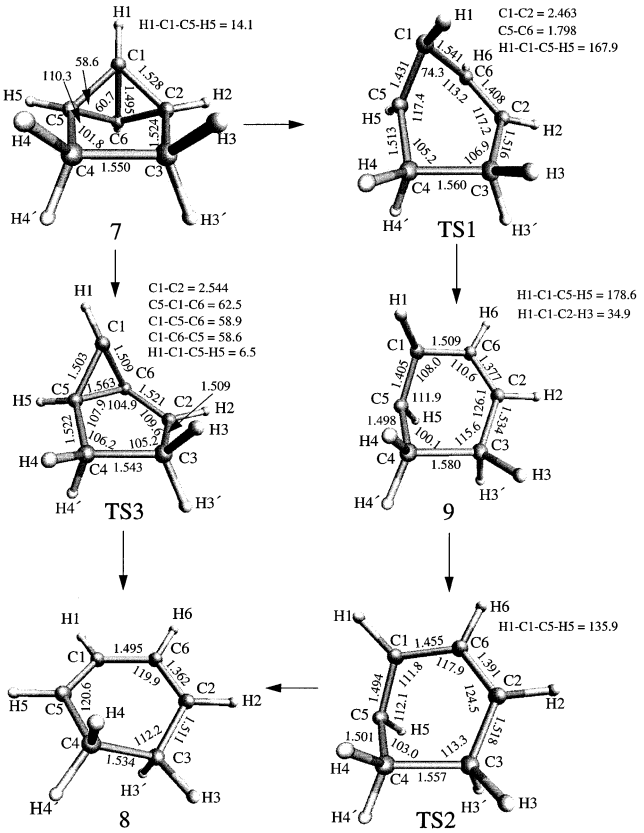

Figure 1. Reaction Schemes for the isomerization of **7** → **8** at the MCSCF/6-31G(d,p) Level.

TABLE 1: Total Energies (Hartrees) and Imaginary Frequencies (cm^{-1})

molecule	MCSCF[a]	QDMCPT2[b]	CCSD(T)[c]	ZPE[d]	frequency[d]
7	−231.91024	−232.61648	−232.77902	0.12886	
TS1	−231.83688	−232.54485	−232.70597	0.12564	446i
9	−231.87891	−232.57481	−232.73530	0.12737	
TS2	−231.86892	−232.56755		0.12453	686i
8	−231.97821	−232.66368	−232.82563	0.12851	
TS3	−231.82293	−232.52599		0.12489	663i

[a] 6-31G(d,p) basis. [b] QDMCPT2/6-31G(d,p)//MCSCF/6-31G(d,p). [c] CCSD(T)/6-311G(d,p)//MP2|6-31G(d,p). [d] MCSCF/6-31G(d,p).

TABLE 2: Activation Energies (Including ZPE; kcal mol^{-1})

molecule	MCSCF[a]	QDMCPT2[b]	CCSD(T)[c]	MP2[d]	B3LYP[d]
TS1	44.9	42.9	42.8	47.4	40.7
TS2	4.6	2.8			
TS3	56.8	54.3			

[a] 6-31G(d,p) basis. [b] QDMCPT2/6-31G(d,p)//MCSCF/6-31G(d,p). [c] CCSD(T)/6-311G(d,p)//MP2/6-31G(d,p). [d] 6-311G(d,p) basis.

This asynchronous step describing the conrotatory conversion of **7** to **9** closely corresponds to the calculated conversion of **1** to **2**.[3] It is worth noting that the lack of symmetry of these steps, with one C−C bond extensively broken at the TS whereas the other is essentially intact, is not in conflict with the Woodward−Hoffmann rules. The orbital diagram **6** clearly lacks symmetry, with the rightmost orbital using only its shaded lobe for interaction, whereas the leftmost orbital uses both of its lobes. Thus, there is no reason that **6** need imply a synchronous bond rearrangement.

The C1−C2 bond is essentially broken in the transition state, with a length of 2.4633 Å. A look at the natural orbital occupation numbers of the MCSCF wave function gives a measure of the amount of biradical character. For a restricted

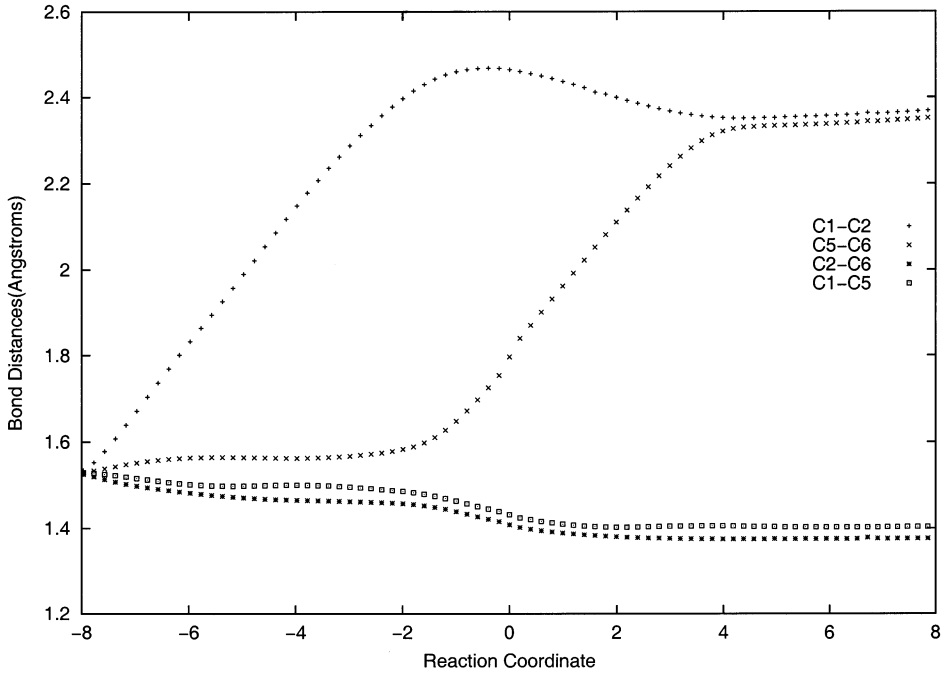

Figure 2. Selected C−C Distances for TS1 IRC at the MCSCF/6-31G(d,p) Level. Reaction Coordinate in units of (amu)$^{1/2}$ bohr.

hartree-fock wave function, the occupation number has a value of two for an occupied orbital and zero for a virtual one. Deviations from zero and two in the MCSCF wave functions offer a measure of diradical character.[3] The occupation numbers of the bonding and antibonding orbitals corresponding to C1−C2 are 1.8222 and 0.1885, respectively. Although there is a moderate amount of configurational mixing, the transition state does not have true diradical character. A similar amount of mixing was found for the **1** → **2** transition state[3] in which the corresponding occupation numbers were 1.8110 and 0.1867, respectively.

The moderate amount of configurational mixing in the transition state suggests that a single-determinant wave function, with correlation correction, might also describe the potential energy surface. We performed calculations at the MP2 and B3LYP levels which gave geometries and energies for this step of the reaction in close agreement to the MCSCF results. The computed IRC at each level of theory confirmed the connection to **9**. The MP2 results gave an $E_a = 47.4$ kcal mol^{-1}, whereas the B3LYP level gives $E_a = 40.7$ kcal mol^{-1} using the 6-311G-(d,p) basis. The single-point energy at the CCSD(T) level gave $E_a = 42.8$ kcal mol^{-1}, using the same basis, which is essentially the same as the corresponding MCQDPT2 result.

The equilibrium geometry and vibrational frequencies of the strained intermediate **9** have been determined at both the MCSCF and single-determinant (HF, MP2, and B3LYP) levels of theory. All of the frequencies are real, confirming this structure as a local minimum on the potential energy surface. The trans double bond produces strain in the molecule as witnessed by the values of several internal coordinates. Included are the C3−C4−C5, C5−C1−C6, and C2−C6−C1 angles, all with values less than normal. On the other hand, the C2−C3−C4 and C3−C2−C6 angles both have values greater than normal. The bond lengths for the double-bonded carbons are slightly longer in the strained counterpart as is C3−C4, whereas the C4−C5 bond length is slightly shorter.

The harmonic frequencies for both **8** and **9**, calculated at the MCSCF and MP2/6-31G(d,p) levels, reveals an interesting difference in the C−H and C−C stretching regions between the two molecules. At the MP2 level, for **8**, the highest four frequencies are spanned by stretches of all four allylic hydrogens, whereas in **9**, the modes are more localized. Interestingly, the third mode, at 3204 cm^{-1}, is comprised of the antisymmetric CH_2 stretch on C4, whereas the fourth and fifth modes are the C−H stretches of the trans double bond which are each localized on one carbon atom. The allylic C−H stretches are also significantly lower in energy in **9**, being red shifted by 39−74 cm^{-1}. Significant deviations also occur in the C═C stretching region between the two isomeric forms. For **8**, there are two modes which span the C═C stretches, one symmetric and the other antisymmetric, whereas in **9**, the two stretches are isolated on individual double bonds. The higher energy mode, at 1604 cm^{-1}, is for the C2═C6 stretch, whereas the trans double bond is coupled with the C4−C5 single bond stretch, which comprise modes at 1555 and 1539 cm^{-1}. The 1555 cm^{-1} mode is composed of almost equal displacements for the three carbons, C1, C4, and C6, whereas the 1539 cm^{-1} mode is much more localized on the double bond carbons C1 and C5, which comprises the trans double bond. Like the allylic C−H stretches, the C═C stretches are significantly lower in energy for **9** with the difference being over 100 cm^{-1}. At the MCSCF level, the normal modes are similar except for modes three and four being switched for the C−H stretches, and the C═C stretch of the trans double bond being isolated at 1564 cm^{-1} and the C═C stretch of the cis double bond being coupled with a CH_2 scissor on C4 at 1623 and 1607 cm^{-1}.

The strain energy of **9** was determined using the homodesmotic reaction model, which we have successfully applied to various strained hydrocarbons of similar size in the past. At the MP2/6-31G(d,p) level, the strain energy is 54.9 kcal mol^{-1}, whereas at the QCISD(T)/6-311+G(2df,p)//MP2/6-31G(d,p) level, it is 55.4 kcal mol^{-1}, using *cis*-2-butene in the homodesmotic reaction. For comparison, we also used *trans*-2-butene in the homodesmotic reaction which raised the strain energy by only 1.3 kcal mol^{-1} to 56.7 kcal mol^{-1} at the QCISD(T) level. As a check of our choice for the homosedmotic reaction, we calculated the strain energy of **8**, which should be close to zero, and obtained a value of 0.4 kcal mol^{-1} at the MP2/6-

311G(d,p) level. Therefore, the presence of the trans double bond contributes about 55−56 kcal mol^{-1} of strain to the ring.

The second step of the mechanism is the rotation about the trans double bond to form **8** from **9**. The transition state (TS2) has been confirmed by calculating the harmonic frequencies (a single imaginary frequency at 686i cm^{-1}), and the IRC is included in the supplemental information. The activation barrier was found to be only 2.8 kcal mol^{-1}, indicative of the strained nature of **9**. TS2 comes early on the PES as shown by the 136° H1−C1−C5−H5 dihedral angle in the transition state compared to 179° in the reactant **9**. The small activation barrier is a consequence of the large amount of ring strain released during the trans double bond rotation, even though the barrier to rotation in ethylene is nearly 70 kcal mol^{-1}. TS2 has strong biradical nature with occupation numbers of 1.337 and 0.664 for the MCSCF natural orbitals comprising the trans π bonding and antibonding orbitals, respectively. Consequently, it is not surprising that we were unable to locate the transition state for this step at the MP2 or B3LYP levels. Starting at the MCSCF optimized geometry for TS2, harmonic frequencies at the MP2 and B3LYP levels include a single imaginary frequency. Following this mode produced a transition state structure that instead lies on an IRC to bicyclo[2.2.0]hex-2-ene(**15**), with an activation barrier of 13.9 kcal mol^{-1} at the CCSD(T)/6-311G-(d,p)//MP2/6-311G(d,p) level. Incidentally, a transition state for the reaction of **9** to **15** was also found at the MCSCF level with an activation barrier of 14.4 kcal mol^{-1} at the MCQDPT2 level. Therefore, π-bond rotation is by far the channel with the lowest barrier from **9**. The reactions from **9** to bicyclo[2.0.0]-hex-2-ene will be included in a subsequent paper.

A reaction channel from **9** to **8** was found at the MP2 level but involved ring opening to give **10** and subsequent ring closure to give **8**. The activation barriers for these two steps are 17.5 and 23.7 kcal mol^{-1} at the CCSD(T)/6-311G(d,p)//MP2/6-311G-(d,p) level, respectively. These barriers are substantially higher than the one for **9** to **8** directly and would not be competitive. An important point here is that the PES is very dependent on the use of a correct wave function, and because of the strong configurational mixing between the π and π^* orbitals for the double bond rotation, a multiconfigurational wave function is necessary.

Probing the surface for a route directly from **7** to **8**, thereby bypassing **9**, we located another transition state (TS3). Following the IRC (supplemental information) confirmed that TS3 leads directly from **7** to **8**. From the structure of TS3, it can be seen that the C1−C5 bond length is 2.544 Å, slightly longer than in TS1. The main differences lie in the C5−C6 distance, which is 1.563 in TS3 compared with 1.798 in TS1, and the H1−C1−C5−H5 dihedral angle which is 6.5° in TS3 and 168° in TS1. It is apparent from the values of the dihedral angles that TS3 leads to **8**; this pathway represents the disrotatory opening. Another interesting difference between TS1 and TS3 is the magnitude of configurational mixing in the wave function. As noted above, TS1 had only a slight degree of configurational mixing; however, the occupation numbers for the bonding and antibonding pair corresponding to the C1−C2 bond in TS3 are 1.06 and 0.94, respectively. This strong mixing reflects the biradical behavior of TS3. It is not surprising that TS3 could not be located at the MP2 or B3LYP single-determinant levels. In fact, starting from the TS3 geometry and calculating the harmonic frequencies at both the MP2 and B3LYP levels gave a single imaginary frequency, implying the structure is in the correct curvature for location of the transition state, but optimizing to the maximum on the saddle point produced a completely different structure, 2-cyclopenten-1-ylmethylene.

TS3 lies 11.4 kcal mol^{-1} higher in energy than TS1, giving an activation barrier of 54.3 kcal mol^{-1} for this channel, significantly higher than TS1 and the formation of **9**. From these calculations, the preferred pathway therefore would be through TS1 and the formation of the intermediate **9**, which rearranges with a very low barrier to form the product **8**.

Conclusions

The thermal isomerization of **7** to form **8** has been investigated using ab initio methods. Two reaction pathways were investigated: a higher energy concerted mechanism which corresponds to a disrotatory process, producing **8** with a barrier of 54.3 kcal mol^{-1}, and a lower-energy two step mechanism proceeding via **9**, with barriers for the two steps of 42.9 and 2.8 kcal mol^{-1}. The intermediate **9** was found to be a relatively shallow minimum on the PES with considerable amount of strain energy due to the trans double bond. Although TS1 can be described at both the single and multideterminantal levels, a multiconfigurational wave function is necessary to adequately describe TS2 and TS3 because of strong configurational mixing in the wave function. In fact, calculations at the MP2 or B3LYP levels give completely different potential energy surfaces, in which **9** instead proceeds to **15** instead of **8**. Only the higher-energy pathway from **9** to **15** is represented using a single-determinant wave function.

Interestingly, the imposition of the two-carbon bridge on bicyclobutane ring opening has little affect on the reaction kinetics compared to **1**. The calculated E_a for conrotatory opening of **1** to **2**, at 41.5 kcal mol^{-1}[3], is barely distinguishable from the E_a for conrotatory opening of **7** to **9**, at 42.9 kcal mol^{-1}. The experimental values for these two processes are also virtually the same and in excellent agreement with the calculated values. The transition state for **1** to **2** is apparently contorted in a way that easily accommodates the addition of a two-carbon bridge between the methylene carbons. The bridge exerts a potent influence after TS1, however, imposing on the strained intermediate **9** a hefty energetic price which the unfettered **2** avoids.

Acknowledgment. The authors gratefully acknowledge financial support from the NSF (EPSCoR), the ONR (initial funding), and the Mississippi Center for Supercomputing Research (MCSCR). The calculations were perfomed on Linux Beawulf clusters (obtained through the NSF EPSCoR program), a SGI Power Challenge and workstation (provided through an NSF equipment grant), and various SGI computers at MCSCR.

Supporting Information Available: Atomic Cartesian coordinates for each structure and intrinsic reaction coordinate plots for each transition state. This material is available free of charge via the Internet at http://pubs.acs.org.

References and Notes

(1) Blanchard, E. P., Jr.; Carncross, A. *J. Am. Chem. Soc.* **1966**, *88*, 487.
(2) Shevlin, P. B.; McKee, M. L. *J. Am. Chem. Soc.* **1988**, *110*, 1666.
(3) Nguyen, K. A.; Gordon, M. S. *J. Am. Chem. Soc.* **1995**, *117*, 3835.
(4) Dewar, M. J. S.; Kirschner, S. J. *J. Am. Chem. Soc.* **1975**, *97*, 2841.
(5) Frey, H. M.; Stevens, I. D. R. *Trans. Faraday Soc.* **1965**, *61*, 90.
(6) Closs, G. L.; Pfeffer, P. E. *J. Am. Chem. Soc.* **1968**, *90*, 2452.
(7) Wiberg, K. B. *Tetrahedron* **1968**, *24*, 1083.
(8) Woodward, R. B.; Hoffmann, R. *The Conservation of Orbital Symmetry*; Verlag Chemie: Weinheim, Germany, 1970; pp 75−78.
(9) Zimmerman, H. E. *Acc. Chem. Res.* **1971**, *4*, 272.

(10) Davis, S. R.; Tan, P. L. *J. Phys. Chem.* **1994**, *98*, 12236.
(11) Walker, J. E.; Adamson, P. A.; Davis, S. R. *Theochemistry* **1999**, *487*, 145.
(12) Wang, H.; Law, C. K. *J. Phys. Chem. B* **1997**, *101*, 3400.
(13) Christl, M.; Bruntrup, G. *Chem. Ber.* **1974**, *107*, 3908.
(14) Christl, M.; Heinemann, U.; Kristof, W. *Chem. Ber.* **1974**, *107*, 3908.
(15) Wiberg, K. B.; Szeimeis, G. *Tetrahedron Lett.* **1968**, *10*, 1235.
(16) Johnson, R. P.; DiRico, K. J. *J. Org. Chem.* **1995**, *60*, 1074.
(17) Bradley, A. Z.; Kociolek, M. G.; Johnson, R. P. *J. Org. Chem.* **2000**, *65*, 7134.
(18) Schmidt, M. W.; Baldridge, K. K.; Boatz, J. A.; Elbert, S. T.; Gordon, M. S.; Jensen, J. H.; Koseki, S.; Matsunaga, N.; Nguyen, K. A.; Su, S. J.; Windus, T. L.; Dupuis, M.; Montgomery, J. A. *J. Comput. Chem.* **1993**, *14*, 1347.
(19) Frisch, M. J.; Trucks, G. W.; Schlegel, H. B.; Scuseria, G. E.; Robb, M. A.; Cheeseman, J. R.; Zakrzewski, V. G.; Montgomery, J. A., Jr.; Stratmann, R. E.; Burant, J. C.; Dapprich, S.; Millam, J. M.; Daniels, A. D.; Kudin, K. N.; Strain, M. C.; Farkas, O.; Tomasi, J.; Barone, V.; Cossi, M.; Cammi, R.; Mennucci, B.; Pomelli, C.; Adamo, C.; Clifford, S.; Ochterski, J.; Petersson, G. A.; Ayala, P. Y.; Cui, Q.; Morokuma, K.; Malick, D. K.; Rabuck, A. D.; Raghavachari, K.; Foresman, J. B.; Cioslowski, J.; Ortiz, J. V.; Stefanov, B. B.; Liu, G.; Liashenko, A.; Piskorz, P.; Komaromi, I.; Gomperts, R.; Martin, R. L.; Fox, D. J.; Keith, T.; Al-Laham, M. A.; Peng, C. Y.; Nanayakkara, A.; Gonzalez, C.; Challacombe, M.; Gill, P. M. W.; Johnson, B. G.; Chen, W.; Wong, M. W.; Andres, J. L.; Head-Gordon, M.; Replogle, E. S.; Pople, J. A. *Gaussian 98*, revision A.11.1; Gaussian, Inc.: Pittsburgh, PA, 1998.
(20) Hehre, W. J.; Ditchfield R.; Pople J. A. *J. Chem. Phys.* **1972**, *56*, 2257.
(21) Nakano, H. *J. Chem. Phys.* **1993**, *99*, 7983).
(22) Nakano, H. *Chem. Phys. Lett.* **1993**, *207*, 372.
(23) Boys, S. F. *Rev. Mod. Phys.* **1960**, *32*, 296.
(24) Gonzalez, C.; Schlegel, H. B. *J. Chem. Phys.* **1989**, *90*, 2154.
(25) Gonzalez, C.; Schlegel, H. B. *J. Phys. Chem.* **1990**, *94*, 5523.
(26) Head-Gordon, M.; Pople, J. A.; Frisch, M. J. *Chem. Phys. Lett.* **1988**, *153*, 503.
(27) Bartlett, R. J.; Purvis, G. D. *Int. J. Quantum Chem.* **1978**, *14*, 516.
(28) Pople, J. A.; Head-Gordon, M.; Raghavachari, K. *J. Chem. Phys.* **1987**, *87*, 5968.
(29) Becke, A. D. *J. Chem. Phys.* **1993**, *98*, 5648.
(30) Lee, C.; Yang, W.; Parr, R. G. *Phys. Rev. B: Condens. Matter* **1988**, *37*, 785.
(31) McLean, A. D.; Chandler, G. S. *J. Chem. Phys.* **1980**, *72*, 5639.
(32) George, P.; Trachtman, M.; Brett, A. M.; Bock, C. W. *J. Chem. Soc., Perkin Trans. 2*, **1977**, 1036.